Supplementary Information

Predicting climate-change impacts on the global glacier-fed stream microbiome

Massimo Bourquin[1,*], Hannes Peter[1], Grégoire Michoud[1], Susheel Bhanu Busi[2], Tyler J. Kohler[3], Andrew L. Robison[1], Mike Styllas[1], Leïla Ezzat[4], Aileen U. Geers[1], Matthias Huss[5,6,7], Stilianos Fodelianakis[1], The Vanishing Glaciers Field Team, Tom J. Battin[1,*]

(1) River Ecosystems Laboratory, Alpine and Polar Environmental Research Center, Ecole Polytechnique Fédérale de Lausanne, EPFL, Lausanne, Switzerland

(2) UK Centre for Ecology and Hydrology, Wallingford, United Kingdom

(3) Department of Ecology, Faculty of Science, Charles University, Prague, Czechia

(4) MARBEC, University of Montpellier, CNRS, Ifremer, IRD, Montpellier, France

(5) Laboratory of Hydraulics, Hydrology and Glaciology (VAW), ETH Zurich, Zurich, Switzerland

(6) Department of Geosciences, University of Fribourg, Fribourg, Switzerland

(7) Swiss Federal Institute for Forest, Snow and Landscape Research (WSL), Birmensdorf, Switzerland

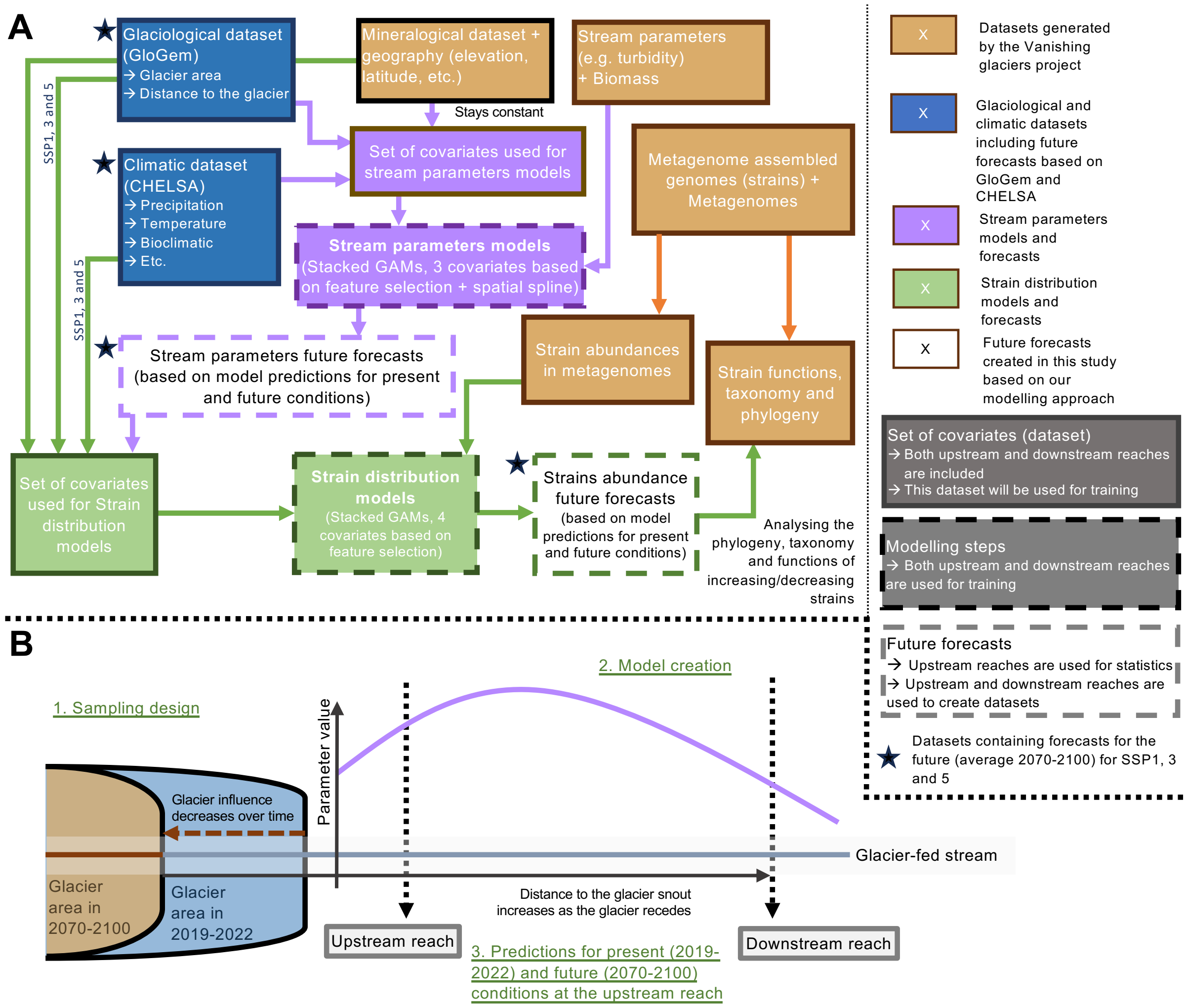

Supplementary Figure 1 Sampling design and model framework (A) A detailed flowchart showing how different datasets were used in our stacked modelling framework. Predictions of glaciological (GloGEM) and climatic (CHELSA) parameter corresponding to SSP1, SSP3 and SSP5 trajectories and geographic, environmental and mineralogical information (obtained through the *Vanishing Glaciers Project*) were used to predict future key stream parameter at the upstream reach. Leveraging present-day differences in MAG abundance between up- and downstream reaches, we then identified individual sets of covariates to train strain-level distribution models. Forecasts of strain-level abundances were then obtained using predictions of selected covariates. These forecasts were used to categorized MAGs into those expected to increase, decrease of remain invariant in terms of abundance in the future. Similarly, individual models were first trained for KOs, and then used to forecast the future functional potential of GFS microbiomes at upstream reaches. Note the different types of input (with or without forecasts), intermediary products, modeling steps and outputs (see legend). The colours differentiate the stream parameters, mineralogical datasets, and metagenomic datasets collected by the Vanishing glaciers project (in beige), the glaciological and climatic datasets gathered from GloGEM and CHELSA (in blue), the modelling of stream parameters (in mauve), and the modelling of Strain distributions and genes (in green). **(B)** Shown is a schematic overview of our sampling design and modeling framework. In each GFS, we sampled microbiomes and measured key environmental factors at an upstream and a downstream reach. The upstream reach was chosen as close as possible to the glacier snout (median distance: 76m) while the downstream reach was located around the terminal moraines (median distance: 706m), typically depicting the last glacial maximum reached during the "Little Ice Age" period (ending about 1850). This design allows for time-for-space substitution and prediction of how environmental drivers at the upstream reach will change as glaciers will recede in the future. Models were thus created using data measured at up- and downstream reaches, predictions of future glacier extent and climate parameter to predict changes in MAG abundances at upstream reaches.

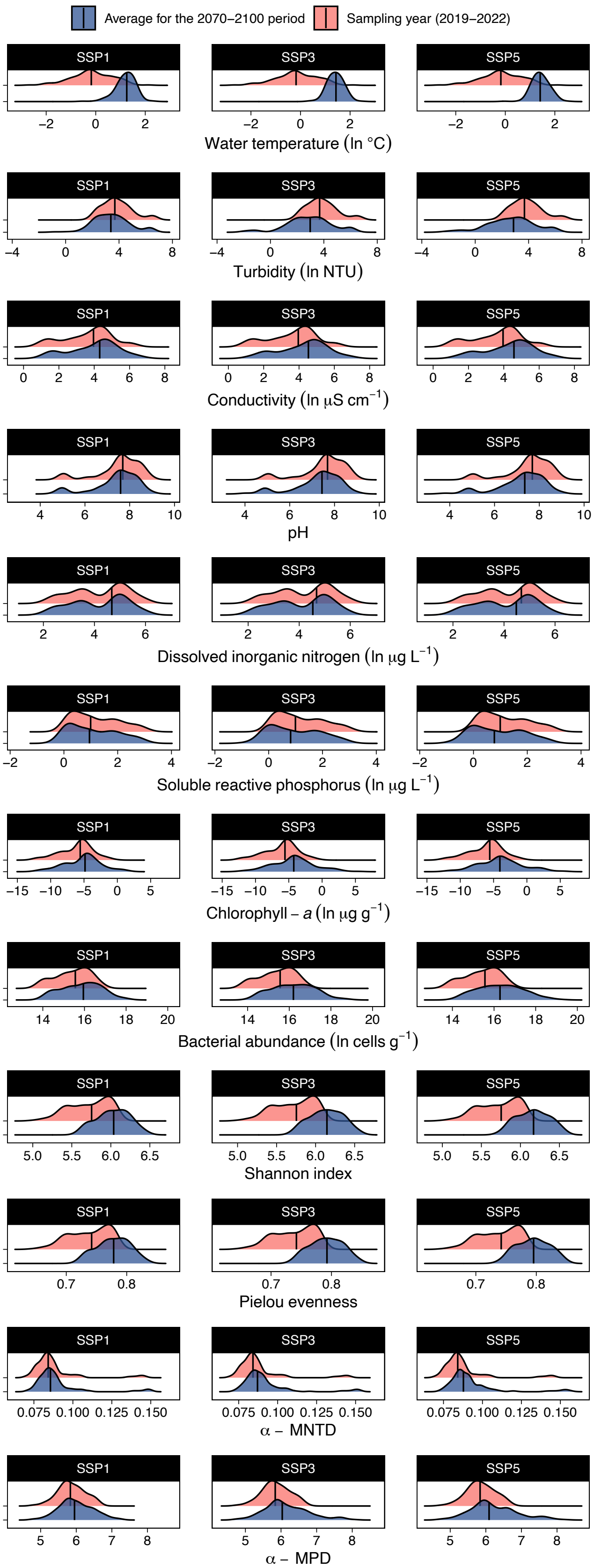

Supplementary Figure 2 Shown are density distributions comparing present-day and future predictions of key environmental covariates, biomass (chlorophyll-a, bacterial abundance) and microbiome-level diversity descriptors for the three different SSP scenarios. Source data are provided as a Source Data file.

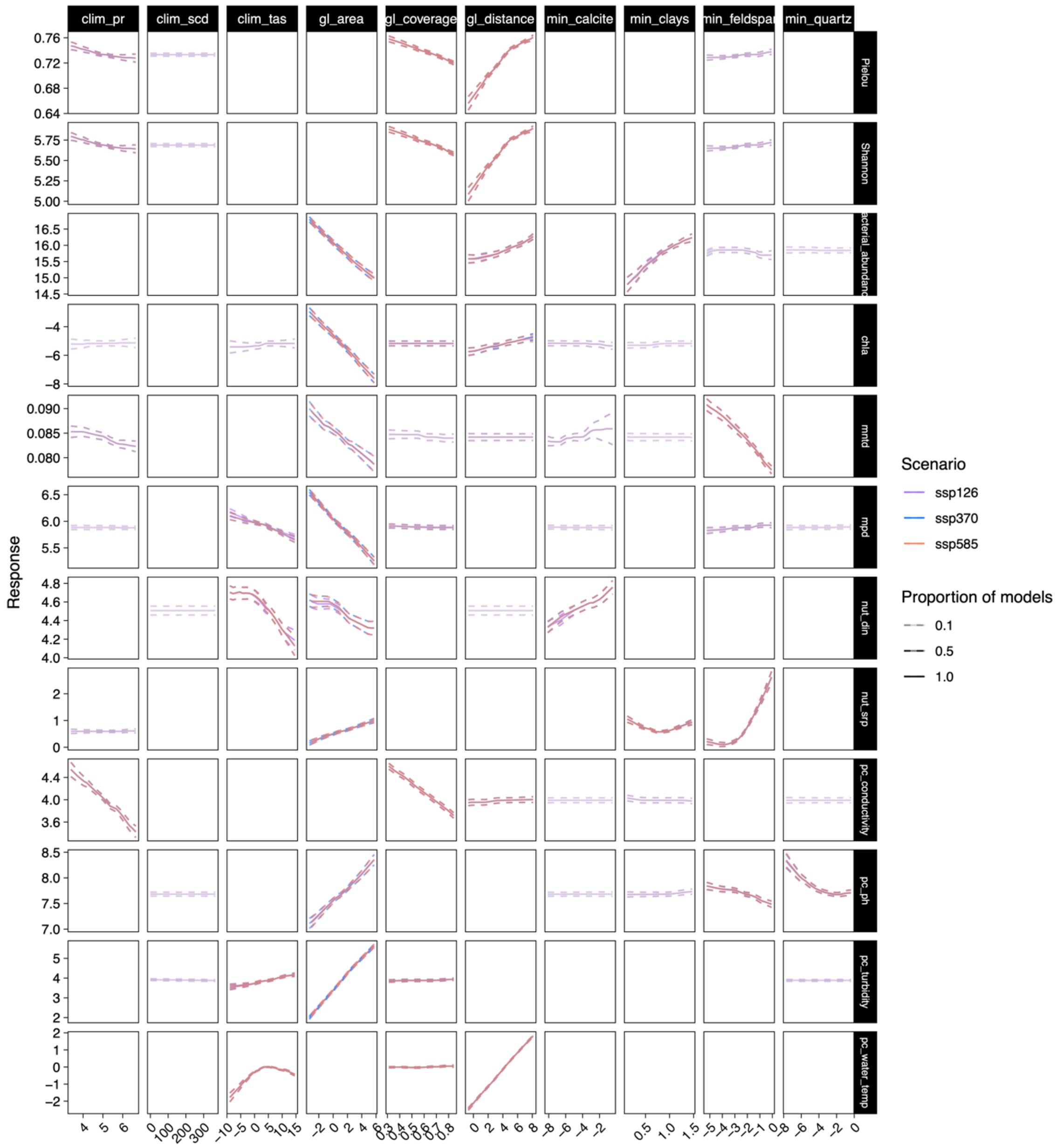

Supplementary Figure 3 Response curve matrix. Depicted are relationships among climatic, glaciological and mineralogical variables (columns) on, covariates used in strain distribution models as well as proxies of biomass (chlorophyll a, bacterial abundance) and diversity (Pilou, Shannon H, mntd, mpd). Response curves (solid line) with confidence intervals (dashed lines) for the three SSPs are shown. Line transparency represents the proportion of stacked models for which the covariate was selected in the feature selection procedure (more important variables are opaquer). Response curves were computed by predicting values for the response variable for each covariate separately through the range of covariate values observed, keeping all other constant at their median. Since spatial splines were used, the median response across sampling sites was computed. The abbreviations for the covariates are the following: gl_dist=distance to the glacier, gl_area=area of the glacier, gl_coverage=coverage of the catchment by the glacier, clim_tas=average monthly temperature, clim_scd=yearly snow cover days, clim_pr=monthly precipitations, min_calcite=calcite content of the sediments, min_clays=clay content of the sediments, min_feldspar=feldspar content of the sediments, min_quartz=quartz content of the sediments, bacterial_abundance =abundance of bacterial cells, chla=mass of chlorophyll-a in the sediments, nut_din=streamwater concentration in dissolved inorganic nitrogen, nut_srp=streamwater concentration in soluble reactive phosphate, pc_conductivity=conductivity of the streamwater, pc_ph=pH of the streamwater, pc_turbidity=turbidity of the streamwater, and pc_water_temp=streamwater temperature. Source data are provided as a Source Data file.

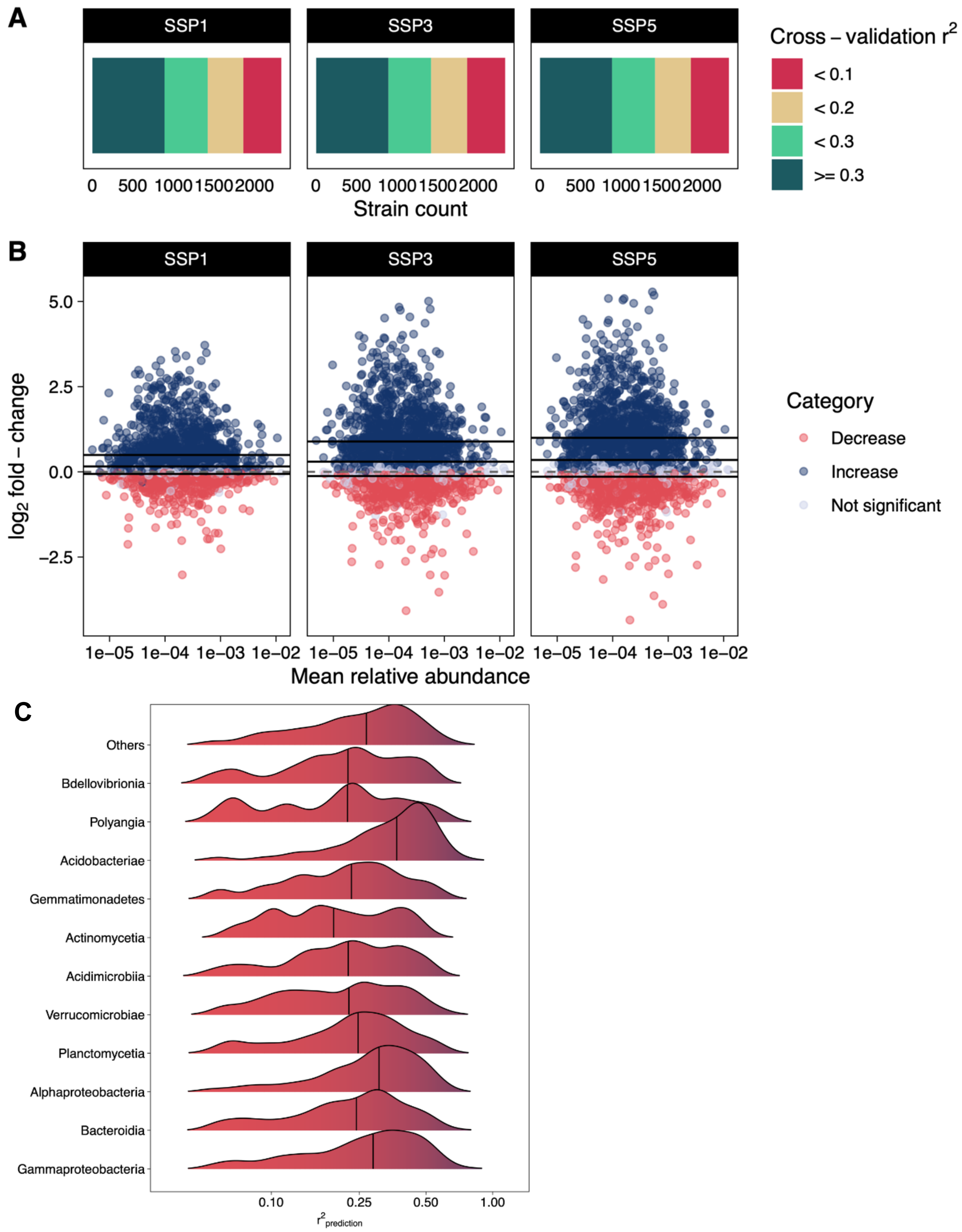

Supplementary Figure 4 Performance of strain distribution models (A) Shown are the distribution of cross-validation results (r^2) for MAG abundances (n=2,333) for the different SSPs. For the majority of MAGs, cross-validation suggested satisfactory model performance (median r^2=0.5). **(B)** Comparison of the predicted magnitude of change in abundance ($\log_2$ fold-change) to current-day mean relative abundance for the different SSPs suggests that MAGs at intermediate relative abundance may respond most strongly (both positively and negatively) to changes in the GFS environmental template. Horizontal lines depict the median and interquartile range of $\log_2$ fold change distributions. The colours differentiate strains that significantly increase/decrease in abundance in future scenarios of climate change. **(C)** Ridge plot depicting the distribution of cross-validation $r^2_{prediction}$ across the 11 most abundant bacterial classes. Source data are provided as a Source Data file.

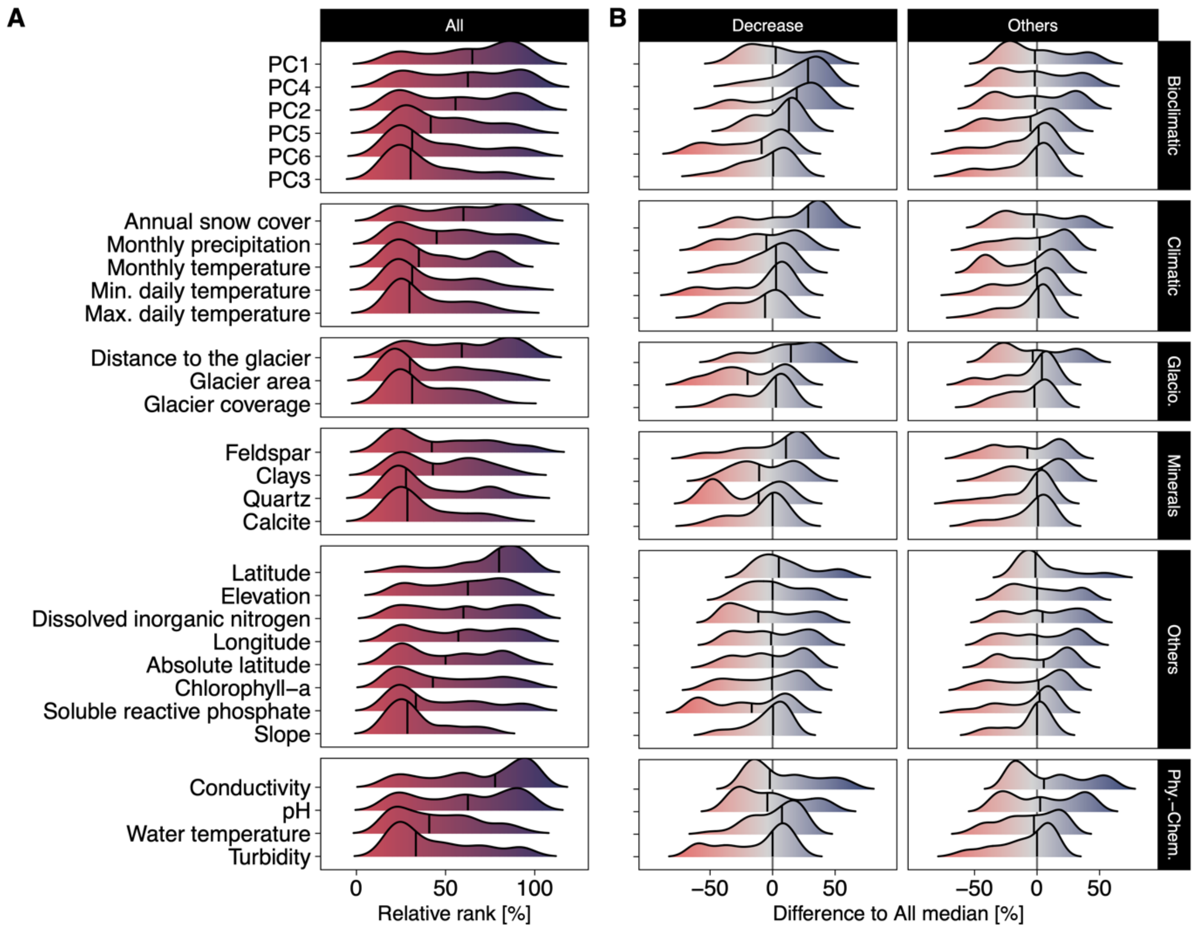

Supplementary Figure 5 Importance of features in the strain distribution models. (A) Displayed are the distribution of covariate ranks in feature selection procedures. Covariates with right-skewed distributions (e.g. streamwater electrical conductivity, pH, bioclimatic PC1) were particularly often ranked among the most important predictors of MAG abundances (irrespective of the direction of change in MAG abundance). Darker colors highlight the relative rank distribution. Vertical lines depict median relative ranks. **(B)** Comparisons of feature rank distributions of MAGs that are predicted to decrease in abundance compared to those that stay invariant or increase (i.e. “others”). Shown are the differences in feature rank to the overall median across all strains. Right-skewed features were particularly important in explaining MAGs predicted to decrease or increase (or remain invariant), respectively. Color gradients highlight the distributions. Vertical lines depict the medians of these distributions. For visual guidance a line through 0 (i.e. no difference to the overall median) is shown. Source data are provided as a Source Data file.

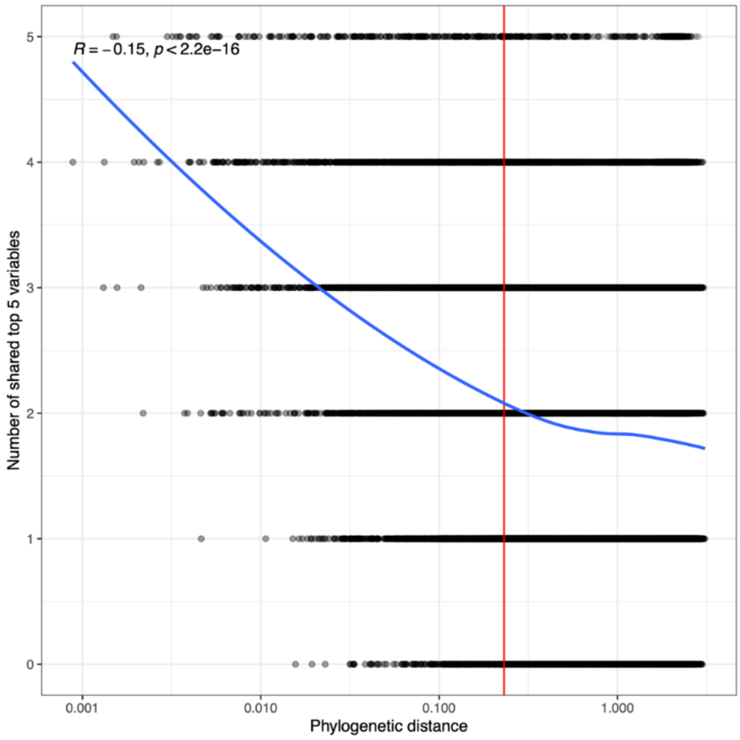

Supplementary Figure 6 Phylogenetic conservatism among important variables. Shown are phylogenetic distances among pairs of MAGs that share 5 or fewer covariates among the five covariates retained by feature selection. The blue line shows a loess fit. For reference, the red vertical line highlights the average within-genus phylogenetic distance. Pairs of closely-related MAGs tended to share more covariates than more distantly related MAGs. The relationship was significant (Spearman Rho = -0.14, p < 0.001). Source data are provided as a Source Data file.

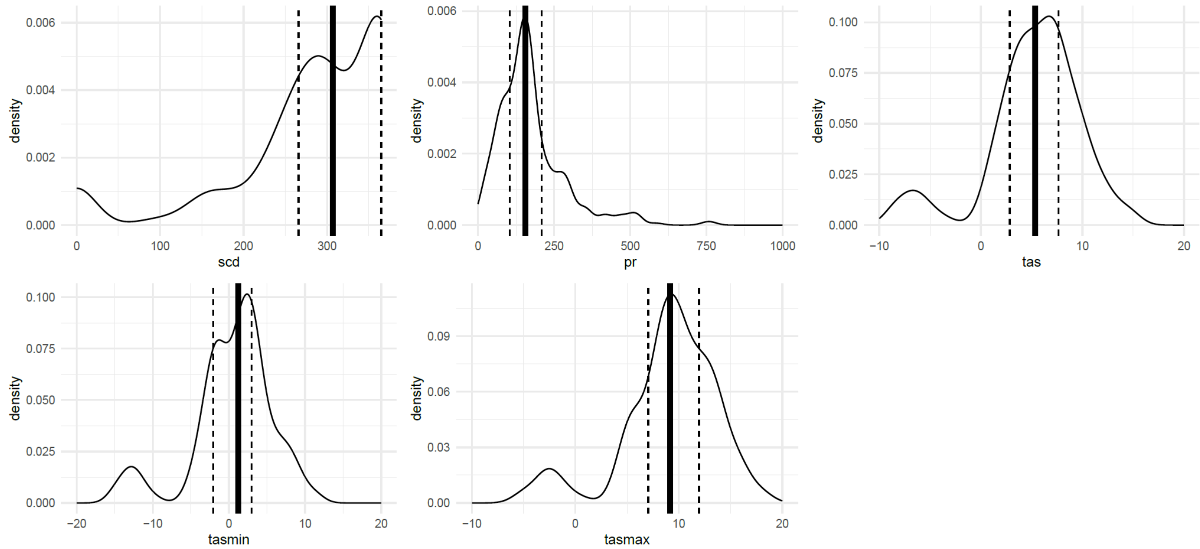

Supplementary Figure 7. Probability density functions of the historical data for the 1981-2010 period for scd (yearly snow cover days), pr (monthly precipitation), tas (average air temperature), tasmin (average minimal daily air temperature), tasmax (average maximal daily air temperature). Median (bold vertical line) and interquartile range (dashed lines) for the 2019-2022 (linearly extrapolated) dataset are shown. Medians and IQR of the extrapolated dataset overlap with historical distributions and do not exhibit extreme values. Source data are provided as a Source Data file.

Supplementary Figure 8 Principal Component Analysis of bioclimatic variables. Shown are PC 1 to 6 for the PCA performed on the 19 bioclimatic variables (clim_bio1 to 19), accounting for more than 95% of the variance. Colours correspond to the mountain ranges, arrows representing the scores of the individual variables were added with the variable names as labels. Source data are provided as a Source Data file.

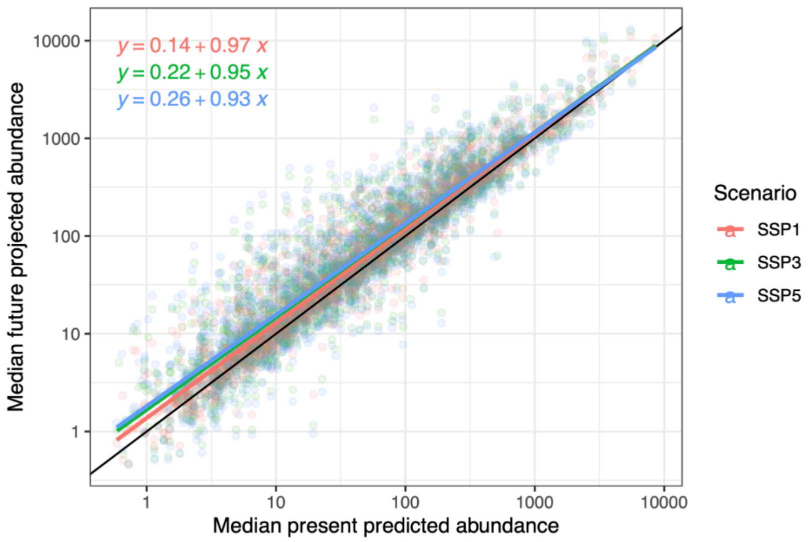

Supplementary Figure 9 Estimate of changes in community evenness. Shown is a scatter plot of the present-day median abundance of MAGs across all GFS and future projected medians under the different SSP scenarios. Linear regressions for each SSP scenario (colored lines) had slopes smaller than one (see linear model equations), indicating that in the future, rare MAGs are predicted be more abundant than currently. This will increase community evenness. The black line represents the 1:1 line. Source data are provided as a Source Data file.

Supplementary Table 1: Provided are sample information including Global Land Ice Measurements from Space (GLIMS) and Randolph Glacier Inventory (rgi) IDs, geographical information and sampling details for the 164 GFS samples at upstream (UP) and downstream (DN) reaches.

Sample ID	***Glacier name***	***GLIMS***	***rgi***	***mountain range***	***Sampling date [DD.MM.YY]***	***latitude [DD]***	***longitude [DD]***	***elevation [m]***
GL1_UP	Franz Josef	G170225 E43495S	RGI60-18.02397	Southern Alps	22.01.19	-43.45	170.1753	470
GL1_DN	Franz Josef	G170225 E43495S	RGI60-18.02397	Southern Alps	22.01.19	-43.4274	170.1734	248
GL2_UP	Victoria	G170174 E43508S	RGI60-18.02270	Southern Alps	25.01.19	-43.4976	170.139	1145
GL2_DN	Victoria	G170174 E43508S	RGI60-18.02270	Southern Alps	25.01.19	-43.4978	170.1291	1093
GL3_UP	Fox	G170162 E43537S	RGI60-18.02375	Southern Alps	26.01.19	-43.5006	170.059	338
GL3_DN	Fox	G170162 E43537S	RGI60-18.02375	Southern Alps	26.01.19	-43.4869	170.0293	226
GL6_UP	Crow	G171511 E42916S	RGI60-18.02896	Southern Alps	30.01.19	-42.9241	171.5137	1362
GL6_DN	Crow	G171511 E42916S	RGI60-18.02896	Southern Alps	30.01.19	-42.9307	171.5185	1118
GL7_UP	White	G171385 E43000S	RGI60-18.02839	Southern Alps	31.01.19	-42.9984	171.3898	1750
GL7_DN	White	G171385 E43000S	RGI60-18.02839	Southern Alps	31.01.19	-42.9963	171.3913	1687
GL8_UP	Marmaduke Dixon	G171383 E42988S	RGI60-18.02823	Southern Alps	02.02.19	-42.9875	171.3904	1629
GL8_DN	Marmaduke Dixon	G171383 E42988S	RGI60-18.02823	Southern Alps	02.02.19	-42.9884	171.3923	1584
GL9_UP	Cahill	G171391 E42978S	RGI60-18.02851	Southern Alps	03.02.19	-42.9824	171.3978	1510
GL9_DN	Cahill	G171391 E42978S	RGI60-18.02851	Southern Alps	03.02.19	-42.9839	171.4025	1253
GL10_UP	Dart	G168609 E44455S	RGI60-18.00686	Southern Alps	08.02.19	-44.4813	168.6059	1090
GL10_DN	Dart	G168609 E44455S	RGI60-18.00686	Southern Alps	08.02.19	-44.4818	168.5979	1042
GL11_UP	Reid	G168623 E44461S	RGI60-18.00676	Southern Alps	09.02.19	-44.4673	168.6216	1587
GL11_DN	Reid	G168623 E44461S	RGI60-18.00676	Southern Alps	09.02.19	-44.4689	168.6193	1486
GL12_UP	Rob Roy	G168718 E44463S	RGI60-18.01013	Southern Alps	10.02.19	-44.4758	168.7268	749
GL12_DN	Rob Roy	G168718 E44463S	RGI60-18.01013	Southern Alps	10.02.19	-44.4803	168.7265	717
GL13_UP	Brewster	G169437 E44072S	RGI60-18.01130	Southern Alps	13.02.19	-44.0819	169.4317	1699
GL13_DN	Brewster	G169437 E44072S	RGI60-18.01130	Southern Alps	13.02.19	-44.0838	169.4305	1655
GL15_UP	Age	G168020 E44606S	RGI60-18.00179	Southern Alps	17.02.19	-44.6121	168.0218	1288
GL15_DN	Age	G168020 E44606S	RGI60-18.00179	Southern Alps	17.02.19	-44.6121	168.0214	1259
GL16_UP	Birch Creek	G170055 E43788S	RGI60-18.01559	Southern Alps	22.02.19	-43.794	170.0643	1320
GL16_DN	Birch Creek	G170055 E43788S	RGI60-18.01559	Southern Alps	22.02.19	-43.7946	170.0674	1206
GL17_UP	Tewaewae	G170073 E43683S	RGI60-18.01881	Southern Alps	23.02.19	-43.6891	170.0822	1236
GL17_DN	Tewaewae	G170073 E43683S	RGI60-18.01881	Southern Alps	23.02.19	-43.6936	170.0849	1006
GL18_UP	Charity	G169924 E43808S	RGI60-18.01835	Southern Alps	26.02.19	-43.8169	169.9252	1208
GL18_DN	Charity	G169924 E43808S	RGI60-18.01835	Southern Alps	26.02.19	-43.8184	169.9279	1113
GL19_UP	Richardson	G169947 E43804S	RGI60-18.01958	Southern Alps	27.02.19	-43.8172	169.9336	1146
GL19_DN	Richardson	G169947 E43804S	RGI60-18.01958	Southern Alps	27.02.19	-43.8239	169.9231	1097
GL20_UP	Mawson	G170508 E43421S	RGI60-18.02348	Southern Alps	01.03.19	-43.418	170.5	1448

GL20_DN	Mawson	G170508 E43421S	RGI60-18.02348	Southern Alps	01.03.19	-43.4074	170.4994	1004
GL21_UP	Shackleton	G170521 E43401S	RGI60-18.02298	Southern Alps	02.03.19	-43.4043	170.5064	1138
GL21_DN	Shackleton	G170521 E43401S	RGI60-18.02298	Southern Alps	02.03.19	-43.406	170.501	982
GL22_UP	Valsorey	G007257 E45892N	RGI60-11.02927	European Alps	25.06.19	45.9166	7.2669	2441
GL22_DN	Valsorey	G007257 E45892N	RGI60-11.02927	European Alps	25.06.19	45.9208	7.257	2387
GL23_UP	Furgg	G007696 E45965N	RGI60-11.02819	European Alps	03.06.20	45.979	7.6868	2735
GL23_DN	Furgg	G007696 E45965N	RGI60-11.02819	European Alps	03.06.20	45.9845	7.6928	2680
GL24_UP	Zmutt	G007639 E45977N	RGI60-11.02739	European Alps	04.06.20	46.0016	7.6511	2317
GL24_DN	Zmutt	G007639 E45977N	RGI60-11.02739	European Alps	04.06.20	46.003	7.6573	2247
GL25_UP	Findelen	G007880 E45990N	RGI60-11.02773	European Alps	05.06.20	46.0108	7.8263	2557
GL25_DN	Findelen	G007880 E45990N	RGI60-11.02773	European Alps	05.06.20	46.0105	7.8199	2508
GL26_UP	Längflue-N	G007860 E46022N	RGI60-11.02742	European Alps	06.06.20	46.031	7.8515	2916
GL26_DN	Längflue-N	G007860 E46022N	RGI60-11.02742	European Alps	06.06.20	46.0318	7.8495	2876
GL27_UP	Arolla (Bas)	G007490 E45965N	RGI60-11.02787	European Alps	08.06.20	45.9901	7.496	2265
GL27_DN	Arolla (Bas)	G007490 E45965N	RGI60-11.02787	European Alps	08.06.20	46.0006	7.4921	2112
GL28_UP	Tsidjiore Nouve	G007450 E45997N	RGI60-11.02755	European Alps	09.06.20	46.016	7.4692	2277
GL28_DN	Tsidjiore Nouve	G007450 E45997N	RGI60-11.02755	European Alps	10.06.20	46.0188	7.4736	2148
GL29_UP	Mont Mine	G007553 E45994N	RGI60-11.02709	European Alps	11.06.20	46.0396	7.5505	2085
GL29_DN	Mont Mine	G007553 E45994N	RGI60-11.02709	European Alps	11.06.20	46.0437	7.5535	1977
GL30_UP	Hohlaub-N	G008004 E46144N	RGI60-11.02526	European Alps	30.06.20	46.1446	7.9939	3081
GL30_DN	Hohlaub-N	G008004 E46144N	RGI60-11.02526	European Alps	30.06.20	46.1449	7.9921	2983
GL31_UP	Schwarzberg	G007922 E46000N	RGI60-11.02746	European Alps	01.07.20	46.0265	7.939	2662
GL31_DN	Schwarzberg	G007922 E46000N	RGI60-11.02746	European Alps	01.07.20	46.0276	7.9397	2659
GL32_UP	"Nuuk east"	G308826 E64132N	RGI60-05.07197	Southwest Greenland	15.07.19	64.1383	-51.1768	613
GL32_DN	"Nuuk east"	G308826 E64132N	RGI60-05.07197	Southwest Greenland	16.07.19	64.1395	-51.1732	550
GL33_UP	"Nuuk middle"	G308801 E64139N	RGI60-05.07202	Southwest Greenland	16.07.19	64.1406	-51.1926	668
GL33_DN	"Nuuk middle"	G308801 E64139N	RGI60-05.07202	Southwest Greenland	16.07.19	64.1418	-51.19	588
GL34_UP	"Nuuk west"	G308763 E64146N	RGI60-05.07208	Southwest Greenland	17.07.19	64.1514	-51.2181	557
GL34_DN	"Nuuk west"	G308763 E64146N	RGI60-05.07208	Southwest Greenland	17.07.19	64.1479	-51.1958	473
GL35_UP	"Nuuk east"	G308916 E64163N	RGI60-05.07210	Southwest Greenland	18.07.19	64.166	-51.0694	757
GL35_DN	"Nuuk east"	G308916 E64163N	RGI60-05.07210	Southwest Greenland	18.07.19	64.1626	-51.059	547
GL36_UP	Aajuitsup Sermia	G308534 E64118N	RGI60-05.07199	Southwest Greenland	21.07.19	64.1211	-51.4805	523
GL36_DN	Aajuitsup Sermia	G308534 E64118N	RGI60-05.07199	Southwest Greenland	21.07.19	64.1262	-51.4901	388
GL37_UP	Teqqiinngallip Sermia	G308542 E64131N	RGI60-05.07207	Southwest Greenland	22.07.19	64.1352	-51.4707	439
GL37_DN	Teqqiinngallip Sermia	G308542 E64131N	RGI60-05.07207	Southwest Greenland	22.07.19	64.1408	-51.4755	249
GL38_UP	Lyngmarksbr ae	G306419 E69295N	RGI60-05.00625	Southwest Greenland	29.07.19	69.2904	-53.571	737
GL38_DN	Lyngmarksbr ae	G306419 E69295N	RGI60-05.00625	Southwest Greenland	29.07.19	69.2815	-53.5372	444

GL39_UP	Chamberlin	G306428 E69317N	RGI60-05.00623	Southwest Greenland	30.07.19	69.3204	-53.5282	468
GL39_DN	Chamberlin	G306428 E69317N	RGI60-05.00623	Southwest Greenland	30.07.19	69.321	-53.4954	332
GL40_UP	Petersen	G306433 E69302N	RGI60-05.00623	Southwest Greenland	31.07.19	69.3013	-53.5476	576
GL40_DN	Petersen	G306433 E69302N	RGI60-05.00623	Southwest Greenland	31.07.19	69.2999	-53.5273	446
GL41_UP	Pjetursson	G306613 E69293N	RGI60-05.00602	Southwest Greenland	01.08.19	69.2955	-53.3929	629
GL41_DN	Pjetursson	G306613 E69293N	RGI60-05.00602	Southwest Greenland	01.08.19	69.3009	-53.4289	395
GL42_UP	Midjirgi	G043172 E43060N	RGI60-12.01262	Caucasus Mountains	11.09.19	43.0936	43.1692	2637
GL42_DN	Midjirgi	G043172 E43060N	RGI60-12.01262	Caucasus Mountains	08.09.19	43.1122	43.1494	2121
GL43_UP	Bezengi	G043084 E43033N	RGI50-12.00014	Caucasus Mountains	09.09.19	43.1057	43.1318	2190
GL43_DN	Bezengi	G043084 E43033N	RGI50-12.00014	Caucasus Mountains	08.09.19	43.1172	43.1493	2037
GL44_UP	"50"/"442"	G043218 E43085N	RGI60-12.00595	Caucasus Mountains	10.09.19	43.0924	43.199	3481
GL44_DN	"50"/"442"	G043218 E43085N	RGI60-12.00595	Caucasus Mountains	11.09.19	43.0941	43.1733	2660
GL45_UP	"50"/"4446"	G043188 E43071N	RGI60-12.01187	Caucasus Mountains	12.09.19	43.0752	43.1743	3027
GL45_DN	"50"/"4446"	G043188 E43071N	RGI60-12.01187	Caucasus Mountains	12.09.19	43.0751	43.1714	2924
GL46_UP	"443"	G043201 E43079N	RGI60-12.00396	Caucasus Mountains	13.09.19	43.0832	43.1839	3154
GL46_DN	"443"	G043201 E43079N	RGI60-12.00396	Caucasus Mountains	13.09.19	43.0858	43.173	2779
GL48_UP	Djankuat	G042766 E43192N	RGI50-12.01132	Caucasus Mountains	18.09.19	43.2034	42.7501	2760
GL48_DN	Djankuat	G042766 E43192N	RGI50-12.01132	Caucasus Mountains	18.09.19	43.2088	42.7396	2642
GL49_UP	Djantugan	G042746 E43195N	RGI60-12.00314	Caucasus Mountains	19.09.19	43.198	42.7382	2799
GL49_DN	Djantugan	G042746 E43195N	RGI60-12.00314	Caucasus Mountains	19.09.19	43.1992	42.7342	2741
GL50_UP	Shkhelda	G042639 E43169N	RGI60-12.00426	Caucasus Mountains	20.09.19	43.1952	42.6484	2364
GL50_DN	Shkhelda	G042639 E43169N	RGI60-12.00426	Caucasus Mountains	20.09.19	43.208	42.6511	2212
GL51_UP	Bashkara	G042727 E43193N	RGI60-12.00849	Caucasus Mountains	22.09.19	43.2099	42.7242	2576
GL51_DN	Bashkara	G042727 E43193N	RGI60-12.00849	Caucasus Mountains	22.09.19	43.2133	42.7148	2466
GL52_UP	Terskol	G042482 E43317N	RGI60-12.00821	Caucasus Mountains	23.09.19	43.291	42.5067	2709
GL52_DN	Terskol	G042482 E43317N	RGI60-12.00821	Caucasus Mountains	23.09.19	43.2753	42.5128	2387
GL53_UP	Garabashi	G042467 E43312N	RGI50-12.00161	Caucasus Mountains	26.09.19	43.2846	42.4788	3059
GL53_DN	Garabashi	G042467 E43312N	RGI50-12.00161	Caucasus Mountains	24.09.19	43.2677	42.4881	2400
GL54_UP	Bolshoy Azau	G042422 E43310N	RGI50-12.00080	Caucasus Mountains	25.09.19	43.2721	42.4468	2561
GL54_DN	Bolshoy Azau	G042422 E43310N	RGI50-12.00080	Caucasus Mountains	25.09.19	43.2654	42.4668	2394
GL55_UP	Irik	G042500 E43332N	RGI50-12.00730	Caucasus Mountains	29.09.19	43.3029	42.5498	2661
GL55_DN	Irik	G042500 E43332N	RGI50-12.00730	Caucasus Mountains	29.09.19	43.292	42.5921	2361
GL56_UP	Sopruju Sevenriy	G041589 E43251N	RGI60-12.00474	Caucasus Mountains	02.10.19	43.2617	41.6102	2104
GL56_DN	Sopruju Sevenriy	G041589 E43251N	RGI60-12.00474	Caucasus Mountains	02.10.19	43.2683	41.6149	1848
GL57_UP	Amanauz	G041628 E43233N	RGI60-12.01112	Caucasus Mountains	03.10.19	43.2622	41.6141	1966
GL57_DN	Amanauz	G041628 E43233N	RGI60-12.01112	Caucasus Mountains	03.10.19	43.2685	41.6151	1848
GL58_UP	Ptish	G041694 E43227N	RGI60-12.00063	Caucasus Mountains	04.10.19	43.2356	41.6929	2347

GL58_DN	Ptish	G041694 E43227N	RGI60-12.00063	Caucasus Mountains	04.10.19	43.2512	41.6916	2113
GL59_UP	"789"	G041670 E43254N	RGI60-12.00053	Caucasus Mountains	05.10.19	43.2668	41.6772	1994
GL59_DN	"789"	G041670 E43254N	RGI60-12.00053	Caucasus Mountains	05.10.19	43.2682	41.6782	1927
GL60_UP	Dvuyazichniy	G041519 E43297N	RGI60-12.00842	Caucasus Mountains	08.10.19	43.2983	41.5478	2109
GL60_DN	Dvuyazichniy	G041519 E43297N	RGI60-12.00842	Caucasus Mountains	08.10.19	43.2989	41.5569	1920
GL61_UP	"San Marco's"	G282003 E00032N	RGI60-16.01343	Ecuadorian Andes	08.02.20	0.0402	-77.9969	4698
GL61_DN	"San Marco's"	G282003 E00032N	RGI60-16.01343	Ecuadorian Andes	08.02.20	0.043	-77.9998	4620
GL62_UP	"Laguna Verde West"	G282007 E00013N	RGI60-16.01345	Ecuadorian Andes	09.02.20	0.0167	-78.0065	4861
GL62_DN	"Laguna Verde West"	G282007 E00013N	RGI60-16.01345	Ecuadorian Andes	09.02.20	0.0157	-78.0079	4780
GL63_UP	Hermoso	G282007 E00013N	RGI60-16.01345	Ecuadorian Andes	10.02.20	0.0107	-78.0068	4661
GL63_DN	Hermoso	G282007 E00013N	RGI60-16.01345	Ecuadorian Andes	10.02.20	0.0104	-78.0068	4647
GL64_UP	"Laguna Verde East"	G282007 E00013N	RGI60-16.01345	Ecuadorian Andes	11.02.20	0.0161	-78.0055	4894
GL64_DN	"Laguna Verde East"	G282007 E00013N	RGI60-16.01345	Ecuadorian Andes	11.02.20	0.0148	-78.0072	4801
GL65_UP	Antisana 12/ Los Crespos	G281855 E00490S	RGI60-16.01339	Ecuadorian Andes	13.02.20	-0.4941	-78.1587	4746
GL65_DN	Antisana 12/ Los Crespos	G281855 E00490S	RGI60-16.01339	Ecuadorian Andes	13.02.20	-0.4942	-78.1588	4739
GL66_UP	Antisana 15 beta	G281855 E00490S	RGI60-16.01339	Ecuadorian Andes	14.02.20	-0.4724	-78.1511	4872
GL66_DN	Antisana 15 beta	G281855 E00490S	RGI60-16.01339	Ecuadorian Andes	14.02.20	-0.4716	-78.1549	4783
GL67_UP	Antisana 15 alpha	G281855 E00490S	RGI60-16.01339	Ecuadorian Andes	15.02.20	-0.4739	-78.1543	4832
GL67_DN	Antisana 15 alpha	G281855 E00490S	RGI60-16.01339	Ecuadorian Andes	15.02.20	-0.4718	-78.1555	4782
GL68_UP	Antisana 14	G281855 E00490S	RGI60-16.01339	Ecuadorian Andes	16.02.20	-0.4778	-78.1582	4791
GL68_DN	Antisana 14	G281855 E00490S	RGI60-16.01339	Ecuadorian Andes	16.02.20	-0.4773	-78.1592	4778
GL69_UP	"Cotopaxi 1. east of refuge"	G281572 E00688S	RGI60-16.02944	Ecuadorian Andes	20.02.20	-0.6672	-78.4341	4913
GL69_DN	"Cotopaxi 1. east of refuge"	G281572 E00688S	RGI60-16.02944	Ecuadorian Andes	20.02.20	-0.6656	-78.4332	4827
GL70_UP	Cotopaxi Glaciar Baja	G281559 E00671S	RGI60-16.02943	Ecuadorian Andes	21.02.20	-0.6681	-78.4405	5048
GL70_DN	Cotopaxi Glaciar Baja	G281559 E00671S	RGI60-16.02943	Ecuadorian Andes	21.02.20	-0.6674	-78.4408	4987
GL71_UP	"Cotopaxi 2. east of refuge"	G281572 E00688S	RGI60-16.02944	Ecuadorian Andes	22.02.20	-0.6673	-78.4316	4867
GL71_DN	"Cotopaxi 2. east of refuge"	G281572 E00688S	RGI60-16.02944	Ecuadorian Andes	22.02.20	-0.666	-78.4306	4803
GL72_UP	"Cotopaxi 3. east of refuge"	G281572 E00688S	RGI60-16.02944	Ecuadorian Andes	23.02.20	-0.6663	-78.4263	4757
GL72_DN	"Cotopaxi 3. east of refuge"	G281572 E00688S	RGI60-16.02944	Ecuadorian Andes	23.02.20	-0.6658	-78.4262	4746
GL73_UP	"Chimborazo Rock Glacier"	G281198 E01465S	RGI60-16.01311	Ecuadorian Andes	27.02.20	-1.4612	-78.7769	4541
GL73_DN	"Chimborazo Rock Glacier"	G281198 E01465S	RGI60-16.01311	Ecuadorian Andes	27.02.20	-1.4605	-78.773	4471
GL74_UP	"Carihuarazo"	G281243 E01403S	RGI60-16.01319	Ecuadorian Andes	29.02.20	-1.4051	-78.7559	4764
GL74_DN	"Carihuarazo"	G281243 E01403S	RGI60-16.01319	Ecuadorian Andes	29.02.20	-1.4062	-78.7566	4725
GL75_UP	"Chimborazo North"	G281194 E01453S	RGI60-16.01308	Ecuadorian Andes	01.03.20	-1.4462	-78.804	4936

GL75_DN	"Chimborazo North"	G281194 E01453S	RGI60-16.01308	Ecuadorian Andes	01.03.20	-1.4456	-78.8039	4935
GL76_UP	Trift VS	G008002 E46138N	RGI60-11.02540	European Alps	02.07.20	46.1358	7.9866	2868
GL76_DN	Trift VS	G008002 E46138N	RGI60-11.02540	European Alps	02.07.20	46.1361	7.9823	2788
GL77_UP	Forno	G009697 E46305N	RGI60-11.02245	European Alps	04.07.20	46.3352	9.7018	2254
GL77_DN	Forno	G009697 E46305N	RGI60-11.02245	European Alps	04.07.20	46.3431	9.7006	2223
GL78_UP	Albigna	G009641 E46297N	RGI60-11.02285	European Alps	05.07.20	46.3131	9.6464	2176
GL78_DN	Albigna	G009641 E46297N	RGI60-11.02285	European Alps	05.07.20	46.3151	9.6468	2165
GL79_UP	Morteratsch	G009641 E46297N	RGI60-11.01946	European Alps	06.07.20	46.4197	9.9338	2176
GL79_DN	Morteratsch	G009641 E46297N	RGI60-11.01946	European Alps	06.07.20	46.4227	9.9335	2063
GL80_UP	Roseg	G009860 E46370N	RGI60-11.02119	European Alps	07.07.20	46.385	9.8419	2276
GL80_DN	Roseg	G009860 E46370N	RGI60-11.02119	European Alps	07.07.20	46.3909	9.8443	2161
GL81_UP	Tschierva	G009886 E46384N	RGI60-11.02051	European Alps	08.07.20	46.4035	9.8695	2326
GL81_DN	Tschierva	G009886 E46384N	RGI60-11.02051	European Alps	08.07.20	46.4122	9.8576	2098
GL82_UP	Silvretta	G010084 E46850N	RGI60-11.00804	European Alps	10.07.20	46.8559	10.0569	2474
GL82_DN	Silvretta	G010084 E46850N	RGI60-11.00804	European Alps	10.07.20	46.8545	10.0542	2430
GL83_UP	Hintereis F.	G010758 E46800N	RGI60-11.00897	European Alps	12.07.20	46.8169	10.7994	2489
GL83_DN	Hintereis F.	G010758 E46800N	RGI60-11.00897	European Alps	12.07.20	46.8199	10.8056	2410
GL84_UP	Niederjoch F.	G010867 E46769N	RGI60-11.00992	European Alps	13.07.20	46.7752	10.8593	2930
GL84_DN	Niederjoch F.	G010867 E46769N	RGI60-11.00992	European Alps	13.07.20	46.7792	10.8603	2829
GL85_UP	Tiefenbach F.	G010927 E46919N	RGI60-11.00674	European Alps	14.07.20	46.9147	10.9339	2929
GL85_DN	Tiefenbach F.	G010927 E46919N	RGI60-11.00674	European Alps	14.07.20	46.9149	10.9356	2870
GL86_UP	Westbreen	G019954 E69491N	RGI60-08.00335	Scandinavian Mountains	07.08.20	69.4734	20.0001	393
GL86_DN	Westbreen	G019954 E69491N	RGI60-08.00335	Scandinavian Mountains	07.08.20	69.4723	20.0078	351
GL87_UP	Midbreen	G019923 E69469N	RGI60-08.03209	Scandinavian Mountains	08.08.20	69.4603	19.9521	517
GL87_DN	Midbreen	G019923 E69469N	RGI60-08.03209	Scandinavian Mountains	08.08.20	69.4584	19.9596	400
GL88_UP	"Southeast of Fugldalsvatnet"	G019849 E69478N	RGI60-08.03199	Scandinavian Mountains	09.08.20	69.4854	19.8359	446
GL88_DN	"Southeast of Fugldalsvatnet"	G019849 E69478N	RGI60-08.03199	Scandinavian Mountains	09.08.20	69.4869	19.8298	385
GL89_UP	"Northwest of Blaaisen"	G019786 E69474N	RGI60-08.03193	Scandinavian Mountains	12.08.20	69.4748	19.7763	946
GL89_DN	"Northwest of Blaaisen"	G019786 E69474N	RGI60-08.03193	Scandinavian Mountains	12.08.20	69.4749	19.7736	939
GL90_UP	Tuftebreen	G007087 E61677N	RGI60-08.01125	Scandinavian Mountains	20.08.20	61.6586	7.1539	859
GL90_DN	Tuftebreen	G007087 E61677N	RGI60-08.01125	Scandinavian Mountains	20.08.20	61.6565	7.1551	792
GL91_UP	Fabergstolbreen	G007202 E61739N	RGI60-08.01133	Scandinavian Mountains	21.08.20	61.7124	7.2921	779
GL91_DN	Fabergstolbreen	G007202 E61739N	RGI60-08.01133	Scandinavian Mountains	21.08.20	61.7132	7.2963	716
GL92_UP	Nigardsbreen	G007099 E61715N	RGI60-08.01126	Scandinavian Mountains	22.08.20	61.6774	7.2073	363
GL92_DN	Nigardsbreen	G007099 E61715N	RGI60-08.01126	Scandinavian Mountains	22.08.20	61.676	7.2118	275
GL93_UP	Boverbreen	G008095 E61549N	RGI60-08.02144	Scandinavian Mountains	23.08.20	61.5564	8.0515	1447

GL93_DN	Boverbreen	G008095 E61549N	RGI60-08.02144	Scandinavian Mountains	23.08.20	61.5571	8.0435	1368
GL95_UP	Storjuvbreen	G008289 E61636N	RGI60-08.00860	Scandinavian Mountains	25.08.20	61.6653	8.2987	1396
GL95_DN	Storjuvbreen	G008289 E61636N	RGI60-08.00860	Scandinavian Mountains	25.08.20	61.6679	8.2997	1357
GL96_UP	Miage	G006846 E45813N	RGI60-11.03005	European Alps	15.09.20	45.7883	6.8885	1812
GL96_DN	Miage	G006846 E45813N	RGI60-11.03005	European Alps	15.09.20	45.7894	6.891	1766
GL97_UP	Très la tête	G006784 E45784N	RGI60-11.03651	European Alps	16.09.20	45.7888	6.7484	2037
GL97_DN	Très la tête	G006784 E45784N	RGI60-11.03651	European Alps	16.09.20	45.7892	6.747	2014
GL98_UP	Mer de glace	G006934 E45883N	RGI60-11.03643	European Alps	17.09.20	45.9357	6.9223	1591
GL98_DN	Mer de glace	G006934 E45883N	RGI60-11.03643	European Alps	17.09.20	45.9375	6.9224	1525
GL99_UP	Pélerins	G006889 E45892N	RGI60-11.03389	European Alps	18.09.20	45.8973	6.8842	2244
GL99_DN	Pélerins	G006889 E45892N	RGI60-11.03389	European Alps	18.09.20	45.8982	6.8827	2205
GL100_UP	Chardon	G006302 E44881N	RGI60-11.03817	European Alps	29.09.20	44.8843	6.2934	2301
GL100_DN	Chardon	G006302 E44881N	RGI60-11.03817	European Alps	29.09.20	44.8863	6.2941	2234
GL101_UP	Des étages	G006263 E44892N	RGI60-11.03694	European Alps	30.09.20	44.8985	6.2624	2440
GL101_DN	Des étages	G006263 E44892N	RGI60-11.03694	European Alps	30.09.20	44.9148	6.2582	2008
GL102_UP	Bonne Pierre	G006341 E44929N	RGI60-11.03810	European Alps	01.10.20	44.9358	6.3183	2436
GL102_DN	Bonne Pierre	G006341 E44929N	RGI60-11.03810	European Alps	01.10.20	44.9387	6.2986	1880
GL103_UP	Lirung	G085556 E28239N	RGI60-15.04045	Himalayas	17.03.21	28.2298	85.56236	4062
GL103_DN	Lirung	G085556 E28239N	RGI60-15.04045	Himalayas	17.03.21	28.22356	85.56226	3989
GL104_UP	Kyimoshung	G085573 E28258N	RGI60-15.04075	Himalayas	18.03.21	28.23401	85.57678	4369
GL104_DN	Kyimoshung	G085573 E28258N	RGI60-15.04075	Himalayas	18.03.21	28.23195	85.57248	4197
GL105_UP	Langtang	G085670 E28312N	RGI60-15.04121	Himalayas	21.03.21	28.23321	85.69581	4488
GL105_DN	Langtang	G085670 E28312N	RGI60-15.04121	Himalayas	21.03.21	28.23187	85.69202	4442
GL106_UP	Langshisha	G085747 E28200N	RGI60-15.04176	Himalayas	22.03.21	28.19602	85.69055	4426
GL106_DN	Langshisha	G085747 E28200N	RGI60-15.04176	Himalayas	22.03.21	28.20647	85.67937	4234
GL107_UP	Shalbachum	G085645 E28262N	RGI60-15.04119	Himalayas	23.03.21	28.21388	85.66135	4255
GL107_DN	Shalbachum	G085645 E28262N	RGI60-15.04119	Himalayas	23.03.21	28.20881	85.66161	4179
GL108_UP	Gangapurna	G083997 E28607N	RGI60-15.04768	Himalayas	04.04.21	28.65324	84.00706	3630
GL108_DN	Gangapurna	G083997 E28607N	RGI60-15.04768	Himalayas	04.04.21	28.6595	84.01666	3508
GL109_UP	Bhakra	G084033 E28623N	RGI60-15.04770	Himalayas	05.04.21	28.64621	84.04721	3543
GL109_DN	Bhakra	G084033 E28623N	RGI60-15.04770	Himalayas	05.04.21	28.64778	84.04729	3496
GL110_UP	Chulu West	G084014 E28747N	RGI60-15.04495	Himalayas	07.04.21	28.74877	83.98823	4829
GL110_DN	Chulu West	G084014 E28747N	RGI60-15.04495	Himalayas	07.04.21	28.74698	83.9882	4762
GL111_UP	"above TP high camp"	G083940 E28774N	RGI60-15.04449	Himalayas	09.04.21	28.77912	83.95431	5093
GL111_DN	"above TP high camp"	G083940 E28774N	RGI60-15.04449	Himalayas	09.04.21	28.78457	83.96045	5003
GL112_UP	Purpung Himal	G084004 E28793N	RGI60-15.04748	Himalayas	10.04.21	28.78145	83.99191	4931
GL112_DN	Purpung Himal	G084004 E28793N	RGI60-15.04748	Himalayas	10.04.21	28.78178	83.98731	4856

GL113_UP	"Icefall Glacier"	G083992 E28799N	RGI60-15.04731	Himalayas	11.04.21	28.78933	83.97688	4893
GL113_DN	"Icefall Glacier"	G083992 E28799N	RGI60-15.04731	Himalayas	11.04.21	28.78656	83.97519	4758
GL114_UP	Chulu Northwest	G084014 E28763N	RGI60-15.04760	Himalayas	12.04.21	28.77362	83.99507	4884
GL114_DN	Chulu Northwest	G084014 E28763N	RGI60-15.04760	Himalayas	12.04.21	28.77479	83.99102	4864
GL115_UP	Nare	G086868 E27821N	RGI60-15.03572	Himalayas	26.04.21	27.8352	86.82957	4528
GL115_DN	Nare	G086868 E27821N	RGI60-15.03572	Himalayas	26.04.21	27.84686	86.82095	4425
GL116_UP	Lhotse	G086915 E27927N	RGI60-15.03742	Himalayas	28.04.21	27.90124	86.87882	4815
GL116_DN	Lhotse	G086915 E27927N	RGI60-15.03742	Himalayas	28.04.21	27.90361	86.8726	4732
GL117_UP	Nuptse	G086868 E27946N	RGI60-15.03735	Himalayas	29.04.21	27.9115	86.86557	4973
GL117_DN	Nuptse	G086868 E27946N	RGI60-15.03735	Himalayas	29.04.21	27.91094	86.86544	4966
GL118_UP	Lhotse Nup	G086891 E27940N	RGI60-15.03731	Himalayas	30.04.21	27.91156	86.88319	4960
GL118_DN	Lhotse Nup	G086891 E27940N	RGI60-15.03731	Himalayas	30.04.21	27.90567	86.87194	4735
GL119_UP	Cholo	G086786 E27909N	RGI60-15.03739	Himalayas	02.05.21	27.91355	86.80015	4391
GL119_DN	Cholo	G086786 E27909N	RGI60-15.03739	Himalayas	02.05.21	27.9122	86.80112	4367
GL120_UP	Aksai	G074544 E42510N	RGI60-13.11414	Pamir & Tien Shan	19.07.21	42.5326	74.5273	3323
GL120_DN	Aksai	G074544 E42510N	RGI60-13.11414	Pamir & Tien Shan	19.07.21	42.5328	74.527	3319
GL121_UP	Top Karagay	G074547 E42486N	RGI60-13.11604	Pamir & Tien Shan	20.07.21	42.5056	74.5048	3334
GL121_DN	Top Karagay	G074547 E42486N	RGI60-13.11604	Pamir & Tien Shan	20.07.21	42.5095	74.5014	3267
GL122_UP	Golubin	G074498 E42454N	RGI60-13.11609	Pamir & Tien Shan	21.07.21	42.4755	74.4829	3371
GL122_DN	Golubin	G074498 E42454N	RGI60-13.11609	Pamir & Tien Shan	21.07.21	42.4778	74.4816	3288
GL123_UP	Tuyuk	G074530 E42461N	RGI60-13.11606	Pamir & Tien Shan	22.07.21	42.473	74.512	3409
GL123_DN	Tuyuk	G074530 E42461N	RGI60-13.11606	Pamir & Tien Shan	22.07.21	42.4806	74.4998	3241
GL124_UP	Tokragula	G074466 E42432N	RGI60-13.11419	Pamir & Tien Shan	23.07.21	42.4383	74.4595	3514
GL124_DN	Tokragula	G074466 E42432N	RGI60-13.11419	Pamir & Tien Shan	23.07.21	42.4439	74.4549	3401
GL125_UP	Tokragula northeast	G074478 E42443N	RGI60-13.11643	Pamir & Tien Shan	24.07.21	42.4399	74.4641	3593
GL125_DN	Tokragula northeast	G074478 E42443N	RGI60-13.11643	Pamir & Tien Shan	24.07.21	42.4444	74.4555	3394
GL126_UP	Petrovski	G072890 E39466N	RGI60-13.13094	Pamir & Tien Shan	31.07.21	39.4713	72.8967	4020
GL126_DN	Petrovski	G072890 E39466N	RGI60-13.13094	Pamir & Tien Shan	31.07.21	39.4818	72.8957	3824
GL127_UP	North of Lenin	G072884 E39433N	RGI60-13.13098	Pamir & Tien Shan	01.08.21	39.4419	72.8983	3970
GL127_DN	North of Lenin	G072884 E39433N	RGI60-13.13098	Pamir & Tien Shan	01.08.21	39.4461	72.9048	3901
GL128_UP	No. 197a	G072967 E39424N	RGI60-13.13252	Pamir & Tien Shan	02.08.21	39.4424	72.9367	3878
GL128_DN	No. 197a	G072967 E39424N	RGI60-13.13252	Pamir & Tien Shan	02.08.21	39.4459	72.9292	3777
GL129_UP	"No. 199a Lenin"	G072928 E39397N	RGI60-13.13251	Pamir & Tien Shan	04.08.21	39.4441	72.9168	3764
GL129_DN	"No. 199a Lenin"	G072928 E39397N	RGI60-13.13251	Pamir & Tien Shan	04.08.21	39.4498	72.9135	3733
GL130_UP	Bordu	G078175 E41813N	RGI60-13.08054	Pamir & Tien Shan	11.08.21	41.8245	78.1545	3838
GL130_DN	Bordu	G078175 E41813N	RGI60-13.08054	Pamir & Tien Shan	11.08.21	41.8313	78.1378	3721
GL131_UP	No. 354	G078164 E41793N	RGI60-13.07064	Pamir & Tien Shan	12.08.21	41.8091	78.1402	3813

GL131_DN	No. 354	G078164 E41793N	RGI60-13.07064	Pamir & Tien Shan	12.08.21	41.811	78.1244	3686
GL132_UP	"Southwest of 354"	G078141 E41787N	RGI60-13.07137	Pamir & Tien Shan	13.08.21	41.8009	78.1335	3869
GL132_DN	"Southwest of 354"	G078141 E41787N	RGI60-13.07137	Pamir & Tien Shan	13.08.21	41.8034	78.1293	3822
GL133_UP	"Road 1"	G077684 E41883N	RGI60-13.06829	Pamir & Tien Shan	14.08.21	41.8879	77.6879	3899
GL133_DN	"Road 1"	G077684 E41883N	RGI60-13.06829	Pamir & Tien Shan	14.08.21	41.8901	77.6894	3796
GL134_UP	"North of road"	G077719 E41916N	RGI60-13.07981	Pamir & Tien Shan	16.08.21	41.9099	77.715	4041
GL134_DN	"North of road"	G077719 E41916N	RGI60-13.07981	Pamir & Tien Shan	16.08.21	41.9076	77.7135	3965
GL135_UP	West Suek/ Batysh Sook	G077749 E41787N	RGI60-13.06974	Pamir & Tien Shan	17.08.21	41.7985	77.7495	3925
GL135_DN	West Suek/ Batysh Sook	G077749 E41787N	RGI60-13.06974	Pamir & Tien Shan	17.08.21	41.7995	77.75	3900
GL136_UP	"2nd west of West Suek"	G077722 E41781N	RGI60-13.06972	Pamir & Tien Shan	18.08.21	41.7929	77.7189	3950
GL136_DN	"2nd west of West Suek"	G077722 E41781N	RGI60-13.06972	Pamir & Tien Shan	18.08.21	41.7943	77.7181	3926
GL137_UP	"West of West Suek"	G077735 E41783N	RGI60-13.06973	Pamir & Tien Shan	19.08.21	41.7925	77.7353	3958
GL137_DN	"West of West Suek"	G077735 E41783N	RGI60-13.06973	Pamir & Tien Shan	19.08.21	41.8019	77.7369	3874
GL138_UP	East Suek	G077771 E41782N	RGI60-13.06975	Pamir & Tien Shan	20.08.21	41.7878	77.7697	4007
GL138_DN	East Suek	G077771 E41782N	RGI60-13.06975	Pamir & Tien Shan	20.08.21	41.7926	77.7672	3909
GL139_UP	"Ski slope"	G077800 E41816N	RGI60-13.06980	Pamir & Tien Shan	21.08.21	41.8182	77.7974	4014
GL139_DN	"Ski slope"	G077800 E41816N	RGI60-13.06980	Pamir & Tien Shan	21.08.21	41.8245	77.7927	3813
GL140_UP	Stanley 003	G029875 E00377N	RGI50-16.01631	Rwenzori Mountains	03.12.21	0.3758	29.8785	4724
GL140_DN	Stanley 003	G029875 E00377N	RGI50-16.01631	Rwenzori Mountains	03.12.21	0.3755	29.8788	4722
GL141_UP	Ventisquiero Yelcho	G287495 E43295S	RGI60-17.11003	Chilean Andes	25.01.22	-43.2891	-72.4689	378
GL141_DN	Ventisquiero Yelcho	G287495 E43295S	RGI60-17.11003	Chilean Andes	25.01.22	-43.2863	-72.4634	312
GL142_UP	Amarillo	G287544 E42827S	RGI60-17.11392	Chilean Andes	26.01.22	-42.8641	-72.4453	498
GL142_DN	Amarillo	G287544 E42827S	RGI60-17.11392	Chilean Andes	26.01.22	-42.8825	-72.4498	430
GL143_UP	"Mocho 1 middle"	G287988 E39929S	RGI60-17.12442	Chilean Andes	30.01.22	-39.9282	-72.0061	1876
GL143_DN	"Mocho 1 middle"	G287988 E39929S	RGI60-17.12442	Chilean Andes	30.01.22	-39.9261	-72	1740
GL144_UP	"Mocho 2 south"	G287988 E39929S	RGI60-17.12442	Chilean Andes	31.01.22	-39.9305	-72.0029	1825
GL144_DN	"Mocho 2 south"	G287988 E39929S	RGI60-17.12442	Chilean Andes	31.01.22	-39.9288	-71.9997	1738
GL145_UP	"Mocho 3 north"	G287988 E39929S	RGI60-17.12442	Chilean Andes	01.02.22	-39.9252	-72.0079	1854
GL145_DN	"Mocho 3 north"	G287988 E39929S	RGI60-17.12442	Chilean Andes	01.02.22	-39.9244	-72.0064	1775
GL146_UP	Pichillancahu e	G288107 E39448S	RGI60-17.12517	Chilean Andes	04.02.22	-39.4407	-71.8884	1817
GL146_DN	Pichillancahu e	G288107 E39448S	RGI60-17.12517	Chilean Andes	04.02.22	-39.4394	-71.879	1740
GL147_UP	Turbio	G288088 E39427S	RGI60-17.12535	Chilean Andes	05.02.22	-39.4315	-71.8797	1748
GL147_DN	Turbio	G288088 E39427S	RGI60-17.12535	Chilean Andes	05.02.22	-39.4271	-71.8786	1703
GL148_UP	"Nevado Chillan 1 east"	G288585 E36836S	RGI60-17.13045	Chilean Andes	08.02.22	-36.8385	-71.4148	2734
GL148_DN	"Nevado Chillan 1 east"	G288585 E36836S	RGI60-17.13045	Chilean Andes	08.02.22	-36.8405	-71.4166	2610
GL149_UP	"Nevado Chillan 2 west"	G288585 E36836S	RGI60-17.13045	Chilean Andes	09.02.22	-36.8451	-71.4253	2273

GL149_DN	"Nevado Chillan 2 west"	G288585 E36836S	RGI60-17.13045	Chilean Andes	09.02.22	-36.8487	-71.4323	2176
GL150_UP	Universidad	G289664 E34607S	RGI60-17.01218	Chilean Andes	11.02.22	-34.7116	-70.3437	2524
GL150_DN	Universidad	G289664 E34607S	RGI60-17.01218	Chilean Andes	11.02.22	-34.7204	-70.3592	2417
GL151_UP	"El Morado"	G289967 E33714S	RGI60-1[15,16]7.1 3710	Chilean Andes	17.02.22	-33.736	-70.0439	3227
GL151_DN	"El Morado"	G289967 E33714S	RGI60-17.13710	Chilean Andes	17.02.22	-33.7691	-70.0441	2731
GL153_UP	"El Morado cliffy"	G289967 E33714S	RGI60-17.13710	Chilean Andes	20.02.22	-33.744	-70.055	3343
GL153_DN	"El Morado cliffy"	G289967 E33714S	RGI60-17.13710	Chilean Andes	20.02.22	-33.744	-70.0527	3293
GL154_UP	"Plomo West"	G290062 E33534S	RGI60-17.13750	Chilean Andes	22.02.22	-33.5739	-69.9214	3495
GL154_DN	"Plomo West"	G290062 E33534S	RGI60-17.13750	Chilean Andes	22.02.22	-33.5825	-69.9175	3359
GL155_UP	"Plomo rock glacier"	G290109 E33559S	RGI60-17.13720	Chilean Andes	23.02.22	-33.6067	-69.9027	3169
GL155_DN	"Plomo rock glacier"	G290109 E33559S	RGI60-17.13720	Chilean Andes	23.02.22	-33.611	-69.9079	3003
GL156_UP	Raven	G210925 E61062N	RGI60-01.08876	Alaska Range	21.06.22	61.066	-149.113	957
GL156_DN	Raven	G210925 E61062N	RGI60-01.08876	Alaska Range	21.06.22	61.07	-149.12	870
GL157_UP	Leanard	G211285 E60812N	RGI60-01.09507	Alaska Range	22.06.22	60.7904	-148.725	233
GL157_DN	Leanard	G211285 E60812N	RGI60-01.09507	Alaska Range	22.06.22	60.784	-148.717	0
GL158_UP	Porcupine	G210738 E60001N	RGI60-01.08618	Alaska Range	23.06.22	59.9992	-149.281	231
GL158_DN	Porcupine	G210738 E60001N	RGI60-01.08618	Alaska Range	23.06.22	59.9999	-149.292	46
GL159_UP	Byron	G211144 E60742N	RGI60-01.09245	Alaska Range	24.06.22	60.7588	-148.852	97
GL159_DN	Byron	G211144 E60742N	RGI60-01.09245	Alaska Range	24.06.22	60.7677	-148.84	57
GL160_UP	Milk	G210925 E61049N	RGI60-01.08875	Alaska Range	25.06.22	61.0454	-149.095	1123
GL160_DN	Milk	G210925 E61049N	RGI60-01.08875	Alaska Range	25.06.22	61.0433	-149.0[17,18]96	1062
GL161_UP	"South of Fourth of July Creek"	G210784 E60074N	RGI60-01.08662	Alaska Range	26.06.22	60.0866	-149.233	538
GL161_DN	"South of Fourth of July Creek"	G210784 E60074N	RGI60-01.08662	Alaska Range	26.06.22	60.088	-149.235	481
GL162_UP	"Second west of Powell"	G212739 E61620N	RGI60-01.23597	Alaska Range	01.07.22	61.6413	-147.268	1520
GL162_DN	"Second west of Powell"	G212739 E61620N	RGI60-01.23597	Alaska Range	01.07.22	61.6433	-147.267	1476
GL163_UP	Powell	G212799 E61568N	RGI60-01.10655	Alaska Range	02.07.22	61.6704	-147.291	949
GL163_DN	Powell	G212799 E61568N	RGI60-01.10655	Alaska Range	02.07.22	61.6736	-147.295	858
GL164_UP	"Third west of Powell"	G212686 E61576N	RGI60-01.10621	Alaska Range	03.07.22	61.6701	-147.309	894
GL164_DN	"Third west of Powell"	G212686 E61576N	RGI60-01.10621	Alaska Range	03.07.22	61.6733	-147.31	848
GL165_UP	Nelchina	G213074 E61558N	RGI60-01.10683	Alaska Range	04.07.22	61.709	-147.074	758
GL165_DN	Nelchina	G213074 E61558N	RGI60-01.10683	Alaska Range	04.07.22	61.7156	-147.072	780
GL166_UP	Sylvester	G212867 E61496N	RGI60-01.23046	Alaska Range	05.07.22	61.6779	-147.067	882
GL166_DN	Sylvester	G212867 E61496N	RGI60-01.23046	Alaska Range	05.07.22	61.683	-147.073	808
GL167_UP	Matanuska	G212412 E61677N	RGI60-01.10557	Alaska Range	06.07.22	61.7752	-147.762	472

GL167_DN	Matanuska	G212412 E61677N	RGI60-01.10557	Alaska Range	06.07.22	61.7877	-147.796	454
GL168_UP	Rainbow Cirque	G214393 E63316N	RGI60-01.24172	Alaska Range	12.07.22	63.3208	-145.611	1496
GL168_DN	Rainbow Cirque	G214393 E63316N	RGI60-01.24172	Alaska Range	12.07.22	63.3247	-145.612	1373
GL169_UP	Castner	G214527 E63453N	RGI60-01.00561	Alaska Range	13.07.22	63.4044	-145.698	816
GL169_DN	Castner	G214527 E63453N	RGI60-01.00561	Alaska Range	13.07.22	63.4024	-145.714	772
GL170_UP	Gulkana	G214573 E63281N	RGI60-01.00570	Alaska Range	14.07.22	63.2551	-145.425	1300
GL170_DN	Gulkana	G214573 E63281N	RGI60-01.00570	Alaska Range	14.07.22	63.2508	-145.445	1174

Supplementary Table 2: Statistics for proximal drivers and biomass models (see the Methods '*Modelling environmental parameters and microbial biomass' for details on the approach*).

Variable	Scenario	Training R^2	Validation $R^2_{prediction}$	N
pc_water_temp	SSP1	0.48369	0.43171	164
pc_water_temp	SSP3	0.48369	0.43171	164
pc_water_temp	SSP5	0.48369	0.43171	164
pc_turbidity	SSP1	0.52241	0.42909	161
pc_turbidity	SSP3	0.52241	0.42896	161
pc_turbidity	SSP5	0.52220	0.42898	161
pc_conductivity	SSP1	0.86952	0.76612	163
pc_conductivity	SSP3	0.86952	0.76612	163
pc_conductivity	SSP5	0.86952	0.76612	163
pc_ph	SSP1	0.70065	0.59972	161
pc_ph	SSP3	0.70051	0.59963	161
pc_ph	SSP5	0.70079	0.60022	161
nut_din	SSP1	0.62278	0.54234	163
nut_din	SSP3	0.62309	0.54245	163
nut_din	SSP5	0.62312	0.54265	163
nut_srp	SSP1	0.58801	0.47281	161
nut_srp	SSP3	0.58802	0.47315	161
nut_srp	SSP5	0.58751	0.47257	161
chla	SSP1	0.58331	0.35455	163
chla	SSP3	0.58316	0.35414	163
chla	SSP5	0.58600	0.35366	163
bacterial_abundance	SSP1	0.44369	0.22970	161
bacterial_abundance	SSP3	0.44476	0.22989	161
bacterial_abundance	SSP5	0.44413	0.22926	161
Shannon	SSP1	0.41185	0.22159	81
Shannon	SSP3	0.41185	0.22159	81
Shannon	SSP5	0.41185	0.22159	81
Pielou	SSP1	0.41157	0.22308	81
Pielou	SSP3	0.41157	0.22308	81
Pielou	SSP5	0.41157	0.22308	81
mntd	SSP1	0.72145	0.51780	81
mntd	SSP3	0.72133	0.51925	81
mntd	SSP5	0.72151	0.51804	81
mpd	SSP1	0.48369	0.43171	81
mpd	SSP3	0.48369	0.43171	81
mpd	SSP5	0.48369	0.43171	81

Supplementary Table 3: Proportion of strains that increase/decrease under future scenarios SSP1, 3 and 5. Median and quartiles of relative changes for all scenarios across the 2333 strains modelled under SSP1, 3 and 5.

Scenario	Increase	Decrease	Not Significant	Q25	Median	Q75
SSP1	0.611	0.266	0.123	-0.061	0.158	0.495
SSP3	0.606	0.265	0.129	-0.124	0.297	0.890
SSP5	0.603	0.268	0.129	-0.143	0.348	0.999

Supplementary Table 4 Phylogenetic signal of future changes ($\log_2$ fold-change) and predictability ($r^2_{prediction}$) for SSP3. The testing was performed using the "lambda" method of the *phytools* R package, yielding log-likelihoods, a lambda value (measure of the phylogenetic signal), and its associated p-value.

Variable	lambda	logl	logl0	p
$\log_2$fold-change	0.9	-2705.0	-3230.1	2.19E-230
$r^2_{prediction}$	0.8	1283.4	1040.3	9.49E-108

Supplementary Table 5 Monophyletic clades with all representatives decreasing in the future under SSP3. The relative phylogenetic depth is derived from the total depth of the tree and the phylogenetic depth of the clade by dividing the latter by the first.

Consensus taxonomy	*n*	*Phylogenetic depth*	*rel. phylogenetic depth*
d__Bacteria;p__Actinobacteriota;c__Actinomycetia;o__Mycobacteriales;f__SCTD01;g__	15	0.952	0.413
d__Bacteria;p__Actinobacteriota;c__Actinomycetia;o__Actinomycetales;f__Microbacteriaceae;g__Lacisediminihabitans;s__	13	1.359	0.163
d__Bacteria;p__Proteobacteria;c__Gammaproteobacteria;o__Burkholderiales;f__Burkholderiaceae;g__LMDS01;s__	8	1.274	0.215
d__Bacteria;p__Actinobacteriota;c__Actinomycetia;o__Actinomycetales;f__Dermatophilaceae;g__UBA4719;s__	8	1.105	0.319
d__Bacteria;p__Acidobacteriota;c__Blastocatellia;o__Pyrinomonadales;f__Pyrinomonadaceae;g__	7	1.055	0.35
d__Bacteria;p__Armatimonadota;c__Chthonomonadetes;o__Chthonomonadales;f__Chthonomonadaceae;g__;s__	7	0.911	0.439
d__Bacteria;p__Proteobacteria;c__Gammaproteobacteria;o__Xanthomonadales;f__Xanthomonadaceae;g__SCMT01;s__	5	1.280	0.211
d__Bacteria;p__Bdellovibrionota;c__Bdellovibrionia;o__Bdellovibrionales;f__Bdellovibrionaceae;g__Pseudobdellovibrio;s__	5	1.368	0.157
d__Bacteria;p__Bacteroidota;c__Bacteroidia;o__Chitinophagales;f__Chitinophagaceae;g__Ferruginibacter;s__	5	1.399	0.138
d__Bacteria;p__Proteobacteria;c__Gammaproteobacteria;o__Burkholderiales;f__Burkholderiaceae;g__Aquabacterium_A;s__	4	1.317	0.188
d__Bacteria;p__Proteobacteria;c__Alphaproteobacteria;o__Sphingomonadales;f__Sphingomonadaceae;g__Sphingomicrobium;s__	4	1.233	0.24
d__Bacteria;p__Myxococcota;c__Polyangia;o__Polyangiales;f__Polyangiaceae;g__	4	1.219	0.249
d__Bacteria;p__Bacteroidota;c__Bacteroidia;o__Sphingobacteriales;f__	4	1.250	0.23
d__Bacteria;p__Bacteroidota;c__Bacteroidia;o__Chitinophagales;f__Chitinophagaceae;g__	4	1.350	0.168
d__Bacteria;p__Chloroflexota;c__Chloroflexia;o__	4	0.460	0.717
d__Bacteria;p__Deinococcota;c__Deinococci;o__Deinococcales;f__Deinococcaceae;g__Deinococcus;s__	4	0.914	0.437
d__Bacteria;p__Proteobacteria;c__Gammaproteobacteria;o__Burkholderiales;f__Burkholderiaceae;g__Rhodoferax;s__	3	1.257	0.225
d__Bacteria;p__Proteobacteria;c__Gammaproteobacteria;o__Burkholderiales;f__Burkholderiaceae;g__Polaromonas;s__	3	1.243	0.234
d__Bacteria;p__Proteobacteria;c__Gammaproteobacteria;o__Burkholderiales;f__Burkholderiaceae;g__	3	0.987	0.392
d__Bacteria;p__Proteobacteria;c__Gammaproteobacteria;o__Burkholderiales;f__Methylophilaceae;g__Methylotenera_A;s__	3	1.279	0.212
d__Bacteria;p__Proteobacteria;c__Gammaproteobacteria;o__Burkholderiales;f__Casimicrobiaceae;g__Casimicrobium;s__	3	1.223	0.246
d__Bacteria;p__Proteobacteria;c__Gammaproteobacteria;o__Xanthomonadales;f__SZUA-5;g__;s__	3	1.196	0.263
d__Bacteria;p__Proteobacteria;c__Gammaproteobacteria;o__Nevskiales;f__Nevskiaceae;g__	3	0.908	0.44
d__Bacteria;p__Proteobacteria;c__Alphaproteobacteria;o__Acetobacterales;f__Acetobacteraceae;g__;s__	3	1.194	0.264
d__Bacteria;p__Proteobacteria;c__Alphaproteobacteria;o__Caulobacterales;f__Caulobacteraceae;g__Phenylobacterium;s__	3	1.251	0.229
d__Bacteria;p__Acidobacteriota;c__Acidobacteriae;o__Bryobacterales;f__Bryobacteraceae;g__;s__	3	1.198	0.262
d__Bacteria;p__Bdellovibrionota;c__Bdellovibrionia;o__Bdellovibrionales;f__Bdellovibrionaceae;g__;s__	3	1.122	0.309
d__Bacteria;p__Myxococcota;c__Polyangia;o__Polyangiales;f__Polyangiaceae;g__	3	1.010	0.377
d__Bacteria;p__Myxococcota;c__Polyangia;o__Polyangiales;f__Polyangiaceae;g__	3	1.194	0.264
d__Bacteria;p__Myxococcota;c__Myxococcia;o__Myxococcales;f__Myxococcaceae;g__JAEUJT01;s__	3	1.113	0.314
d__Bacteria;p__Bacteroidota;c__Bacteroidia;o__Chitinophagales;f__Chitinophagaceae;g__Ferruginibacter;s__	3	1.369	0.156
d__Bacteria;p__Bacteroidota;c__Bacteroidia;o__Chitinophagales;f__Chitinophagaceae;g__Ferruginibacter;s__	3	1.408	0.132
d__Bacteria;p__Bacteroidota;c__Bacteroidia;o__Chitinophagales;f__Saprospiraceae;g__M3007;s__	3	1.401	0.137
d__Bacteria;p__Planctomycetota;c__Planctomycetia;o__Isosphaerales;f__Isosphaeraceae;g__;s__	3	1.123	0.308
d__Bacteria;p__Verrucomicrobiota;c__Verrucomicrobiae;o__Verrucomicrobiales;f__Verrucomicrobiaceae;g__VFKE01;s__	3	1.217	0.25
d__Bacteria;p__Actinobacteriota;c__Acidimicrobiia;o__Acidimicrobiales;f__RAAP-2;g__RAAP-2;s__	3	1.294	0.203
d__Bacteria;p__Cyanobacteria;c__Cyanobacteriia;o__Cyanobacteriales;f__Microcoleaceae;g__Microcoleus;s__	3	1.024	0.369

Supplementary Table 6: Top KEGG orthologous groups highlighted in the phylogenetic random forest analysis. The 'n' column represents in how many of the 10 cross-validation folds the KO was significant.

KEGG KO	n	Description
K03117	10	sec-independent protein translocase protein TatB - Importance for cold-shock in *S. oneidensis* (https://journals.asm.org/doi/full/10.1128/jb.01908-05)
K03168	10	DNA topoisomerase I topA - cold sensitivity of mutants lacking this gene in *E. coli* (https://www.jbc.org/article/S0021-9258(20)76598-1/fulltext)
K02860	9	16S rRNA processing protein RimM - expression linked with the cold-adaptation RbfA gene (https://www.annualreviews.org/doi/pdf/10.1146/annurev-biochem-062608-160432)
K03814	9	monofunctional glycosyltransferase mtgA - peptidogylacan maturation (https://febs.onlinelibrary.wiley.com/doi/abs/10.1016/0014-5793%2896%2900809-5)
K13288	9	oligoribonuclease orn, REX2, REXO2 - associated with biofilm formation (https://www.pnas.org/doi/full/10.1073/pnas.1507245112)
K00140	8	malonate-semialdehyde dehydrogenase (acetylating) / methylmalonate-semialdehyde dehydrogenase mmsA, iolA, ALDH6A1 - differentially expressed at cold temperatures in *Psychrobacter* (https://ami-journals.onlinelibrary.wiley.com/doi/full/10.1111/1462-2920.13578)
K00847	8	fructokinase scrK
K01800	8	maleylacetoacetate isomerase maiA, GSTZ1
K02339	8	DNA polymerase III subunit chi holC
K03179	8	4-hydroxybenzoate polyprenyltransferase ubiA
K03216	8	tRNA (cytidine/uridine-2'-O-)-methyltransferase trmL, cspR - tRNA and cold adaptation (https://www.mdpi.com/2218-273X/7/2/35)
K03558	8	membrane protein required for colicin V production cvpA - bacteriocin (https://journals.asm.org/doi/full/10.1128/mmbr.00036-06)
K03821	8	poly[(R)-3-hydroxyalkanoate] polymerase subunit phaC, phbC - PHAs in the Baltic sea, adaptation to cold (https://link.springer.com/article/10.1007/s00792-014-0699-9, https://link.springer.com/article/10.1007/s00792-014-0699-9#ref-CR7)
K04760	8	transcription elongation factor greB
K06195	8	ApaG protein apaG
K07396	8	putative protein-disulfide isomerase, participates in the insertion of lipopolysaccharides in the outer membrane (https://www.sciencedirect.com/science/article/pii/S0021925820526628?via%3Dihub)
K07518	8	hydroxybutyrate-dimer hydrolase
K09748	8	ribosome maturation factor rimP - associated with the cold-adaptation RbfA gene, important at higher temperatures (https://www.sciencedirect.com/science/article/pii/S0022283608016148, https://www.microbiologyresearch.org/content/journal/micro/10.1099/mic.0.052209-0)
K11443	8	two-component system, cell cycle response regu[17,20–22]lator DivK
K14472	8	succinyl-CoA:(S)-malate CoA-transferase subunit B, smtB - carbon metabolism
K14540	8	ribosome biogenesis GTPase A rbgA

Supplementary Table 7: Enrichment analysis of the KEGG orthologous groups associated with the strains forecasted to decrease. The statistical significance and odds ratio were assessed by performing a two-sided Fisher test on the KEGG categories, testing for an enrichment in significant KOs in the category compared to all other categories. Adjusted p-values were obtained by applying the Bonferroni correction.

Pathway	Odds ratio	p-value	Adjusted p-value
09101 Carbohydrate metabolism	2.20	5.7E-12	0.00000
09102 Energy metabolism	1.80	0.00016	0.00284
09103 Lipid metabolism	0.98	1	1
09104 Nucleotide metabolism	1.65	0.02634	0.47417
09105 Amino acid metabolism	1.30	0.06849	1
09106 Metabolism of other amino acids	1.33	0.28995	1
09107 Glycan biosynthesis and metabolism	0.63	0.14770	1
09108 Metabolism of cofactors and vitamins	1.19	0.35992	1
09109 Metabolism of terpenoids and polyketides	1.31	0.27840	1
09110 Biosynthesis of other secondary metabolites	0.81	0.62851	1
09111 Xenobiotics biodegradation and metabolism	1.17	0.44283	1
09121 Transcription	2.61	0.22741	1
09182 Protein families: genetic information processing	0.66	0.00037	0.00675
09183 Protein families: signaling and cellular processes	0.42	8.5E-11	1.5E-09
09191 Unclassified: metabolism	0.87	0.51772	1
09192 Unclassified: genetic information processing	0.55	0.31008	1
09193 Unclassified: signaling and cellular processes	0.41	0.10410	1
09194 Poorly characterized	0.31	0.00169	0.03050

Supplementary Table 8: Random forest analysis hyperparameter random grid.

Parameter	values
Regularization.factor	0.2,0.4,0.6,0.8,1
Num.trees	250,500,750,1000,1500
Max.depth	5,15,30,50
Regularization.usedepth	0.0263429482376568
mtry	20,30,40,50
splitrule	'hellinger','extratrees','gini'
Sample.fraction	0.5,0.6,0.7,0.8